



Comparison study on the adsorption performance of methylene blue and congo red on Cu-BTC

Jue Hu, Wei Dai*, Xiaoyang Yan

College of Chemistry and Life Science, Zhejiang Normal University, Zhejiang Province, Jinhua 321004, P.R. China, Tel. +86 0579 82282269; email: daiwei@zjnu.edu.cn (W. Dai)

Received 13 March 2014; Accepted 10 November 2014

ABSTRACT

Cu-BTC, one of the metal–organic frameworks (MOFs), has been applied to remove the cationic dye methylene blue (MB) and anionic dye methyl orange (CR) from contaminated water. Liquid phase adsorption experiments were conducted and the maximum adsorptive capacity was determined. Various conditions were evaluated, including initial dye concentration, contact time, solution pH, and temperature. The Langmuir and Freundlich adsorption models were used to describe the equilibrium isotherm and isotherm constant calculation. It was found that the Cu-BTC adsorption capacities of MB and CR are much higher than those of the other types of MOFs and adsorbents. Maximum equilibrium adsorption capacities of 143.27 and 877.19 mg/g for MB and CR were achieved. Three simplified kinetic models including pseudo-first-order, pseudo-second-order, and intra-particle diffusion equations were used to investigate the adsorption process. The pseudo-second-order equation was followed for adsorption of MB and CR on Cu-BTC. Temperature-dependent adsorption behaviors of MB and CR show that the adsorption is a spontaneous and endothermic process accompanying an entropy increase. This work indicates that Cu-BTC could be employed as an effective adsorbent in the removal of the textile dyes from effluents.

Keywords: Adsorption performance; Methylene blue; Congo red; Cu-BTC

1. Introduction

Dye is used in many industries such as food, paper, carpets, rubbers, plastics, cosmetics, and textiles. These dyes are common water pollutants and they may be frequently found in trace quantities in industrial wastewater [1]. Their presence in water, even at low concentrations, is highly visible and undesirable. When these colored effluents enter rivers or any surface water system they upset biological activity and aquatic ecosystem. These colored compounds are

not only aesthetically displeasing but also inhibiting sunlight penetration into these water bodies [2]. Ground water is also affected by these pollutants because of leaching from the soil. Many dyes are difficult to degrade due to their complex aromatic structure and they tend to persist in the environment creating serious water quality and public health problems such as allergic dermatitis, skin irritation, cancer, and mutation [2]. Furthermore, these dyes are toxic to micro-organisms and may cause direct destruction or inhibition of their catalytic capabilities.

The methylene blue (MB) and congo red (CR) are the typical function dyes, and have been widely used

*Corresponding author.

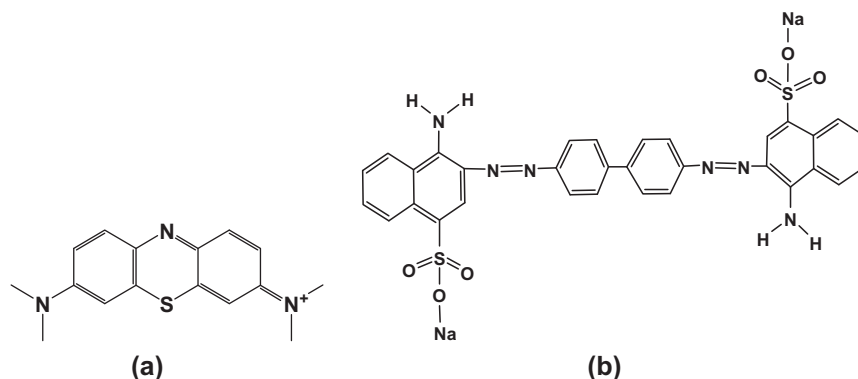


Fig. 1. Chemical structures of MB (a) and CR (b).

in textile, printing, paper, food, and pharmaceutical industries [3,4]. The structures of MB and CR are shown in Fig. 1. They can cause eye burns which may be responsible for permanent injury to the eyes of human and animals. On inhalation, they can give rise to short periods of rapid or difficult breathing while ingestion through the mouth produces a burning sensation and may cause nausea, vomiting, profuse sweating, mental confusion, and methemoglobinemia [3,4]. Therefore, CR and MB containing effluents have to be sufficiently removed before they are discharged into the water bodies.

Adsorption technique is by far the most simple and effective method owing to advantages of being less energy intensive, easy to regenerate, having fast adsorption/desorption kinetics, and low-cost of solid adsorbent [5,6]. Common adsorbent materials are: activated alumina, silica gel, metal hydroxides, molecular sieves, activated carbon, and metal–organic frameworks (MOFs). In particular, MOFs materials have attracted considerable attention recently due to the possibility of designing a structure with a particular pore size and shape from multifunctional ligands and metal ions. The major applications currently of MOFs focus on gas storage, catalysis, separations, as carriers for nanomaterials, and drug delivery [7–9]. However, the study about the removal of dyes from aqueous solution adsorption by MOFs is still scarce. Especially, no attempts have been made to compare the adsorption of MB and CR by using MOFs. Among all kinds of MOFs, the most popular and most investigated MOF so far is Cu-BTC ($\text{Cu}_3(\text{BTC})_2$, BTC: 1,3,5-benzenetricarboxylate) also known as HKUST-1 [10]. The paddle wheel complex built from the axial Cu^{2+} ion and 1,3,5-benzenetricarboxylic acid, is very interesting for its easy preparation, flexibility, and open metal site. Due to its good thermal stability and its well-defined

structure, it therefore may be favorable for the removal of MB and CR dyes from wastewater.

In this paper, we compare the adsorption properties for the typical cationic dyes MB and CR over Cu-BTC because the adsorption can be understood much by a comparison between the two adsorbates. Adsorptive equilibrium isotherms, kinetics, and thermodynamics were processed to understand the adsorption mechanism of the dyes molecules onto the Cu-BTC. Moreover, this work will also help in comparison with adsorption equilibrium results between simulations and experiments.

2. Materials and methods

2.1. Materials

An aqueous stock solution of MB was prepared by dissolving MB ($\text{C}_{16}\text{H}_{18}\text{ClN}_3\text{S}$, MW: 373.9, Sigma-Aldrich) in deionized water. It was soaked slowly to make sure that all the MB powder has been dissolved in distilled water. This stock solution was stored for further purpose. This entire step has been repeated with CR ($\text{C}_{32}\text{H}_{22}\text{N}_6\text{Na}_2\text{O}_6\text{S}_2$, MW: 696.66, Sigma-Aldrich) instead of MB. The maximum wavelength for MB is 668 nm whereas CR is 500 nm. All other reagents were of analytical reagent grade.

2.2. Preparation of Cu-BTC

The Cu-BTC was prepared by the method following the detailed description given in the literature [11]. Details of the preparation procedure are: $\text{Cu}(\text{NO}_3)_2 \cdot 3\text{H}_2\text{O}$ (5 g, 0.021 mol) and H_3BTC (2.5 g, 0.012 mol) were dissolved in 300 mL of solvent consisting of equal amounts of DMF, ethanol, and deionized water by ultrasonication. The solution was placed in an oven and heated to 358 K for 20 h. The blue

product was isolated, rinsed with 50 mL DMF for three times, and immersed in absolute ethanol every 24 h for 72 h. Finally, the blue product was heated to 393 K for 24 h in vacuum.

2.3. Characterization of Cu-BTC

X-ray diffraction data were recorded from a Bruker D8 Advance X-ray diffractometer with Cu K α radiation ($\lambda = 1.542 \text{ \AA}$). Scanning electron microscopy (SEM) images were obtained from a scanning electron microscope (Philips PW 3040/60) operated at 20 kV. Prior to the observation, the sample was sputter-coated with a gold layer to increase their conductivity. Specific surface areas and pore volumes were determined by N₂ adsorption. An automated adsorption apparatus (Micromeritics, ASAP2020) was used for these measurements. N₂ adsorption was carried out at liquid N₂ temperature (77 K). The specific surface areas were calculated using the BET equation by assuming a section area of nitrogen molecule to be 0.162 nm². The total pore volume was estimated to be the liquid N₂ volume at a relative pressure of 0.99. The pore size distribution was calculated by density functional theory (DFT). The morphological features and surface characteristics of the samples were obtained from SEM using a Hitachi S-4800 scanning electron microscope at an accelerating voltage of 15 kV. The samples were coated with platinum by electro-deposition under vacuum prior to analyses.

2.4. Batch adsorption experiments

Adsorption measurements on Cu-BTC were carried out in batches. A desired amount of the adsorbent was added to 50 mL of the MB and CR solution with various initial concentrations (10–800 mg/L). The desired pH was achieved by adjustment with 0.1 M HCl or 0.1 M NaOH. The mixture was stirred magnetically at certain temperature (303, 313, and 323 K) and 150 rpm, and samples were withdrawn from the experimental flask at pre-determined time intervals until the adsorption equilibrium was reached. Next, the dye solution was separated from the adsorbent by centrifugation (TGL-16G, Zhejiang Nade Company) at 8,000 rpm for 20 min. The supernatants were filtered using a Millex-HN filter (Millipore 0.45 mm, Zhejiang Nade Company) to ensure that the solutions were free of adsorbent particles prior to measuring the residual dye concentration. It was found that the calibration curves were very reproducible and linear over the concentration range used in this work. The adsorbed amount of MB and CR at equilibrium, q_e (mg/g), was calculated by the following expression:

$$q_e = \frac{(C_0 - C_e) \cdot V}{W} \quad (1)$$

where C_0 and C_e (mg/L) are the initial and equilibrium concentrations of MB and CR solution, respectively, V (L) is the volume of solution, and W (g) is the weight of Cu-BTC used.

3. Results and discussion

3.1. Characterization of the Cu-BTC

The as-prepared adsorbent Cu-BTC was proven by examinations with XRD, SEM analyses, and N₂ adsorption at 77 K. The characterization results were shown in Fig. 1. As can be known from Fig. 2(A) and (B), the Cu-BTC sample shows type-I adsorption isotherm according to the IUPAC classification [12]. The BET surface area and pore volume of Cu-BTC sample were 1189.81 m²/g and 0.43 cm³/g, respectively. The pore size distributions calculated by DFT prove that the pore size of the sample range from 1 to 2 nm. The high surface area of the Cu-BTC provides the huge capacity for dye molecules' adsorption inside the pore structure. Fig. 2(C) shows the XRD patterns of the resulting products. All diffraction peaks can be indexed to crystalline Cu-BTC [11], and no obvious peaks of impurities can be detected in the XRD patterns. Small variations in intensity can be ascribed to a different degree of hydration. Moreover, sharpness and high intensity of peaks indicate high crystallinity of the prepared bulk materials, which is in accordance with the SEM (Fig. 2(D)) image of the Cu-BTC sample.

3.2. Influence of initial pH values

It is known that the solution pH can affect the surface charge of the adsorbent, the degree of ionization of different pollutants, the dissociation of functional groups on the active sites of the adsorbent as well as the structure of the dye molecule. Thus, the solution pH is an important parameter during the dye adsorption process. Fig. 3 shows the effect of pH value on the adsorption of MB and CR onto Cu-BTC. The adsorption of MB and CR onto Cu-BTC are intimately dependent on solution pH. The adsorption capacities of MB and CR increase with increasing solution pH from 4 to 7. However, the adsorption capacities decreased significantly when the pH of the system was increased, and remained nearly constant over the pH values of 7–9. The results are similar to previously reported in the literature [2].

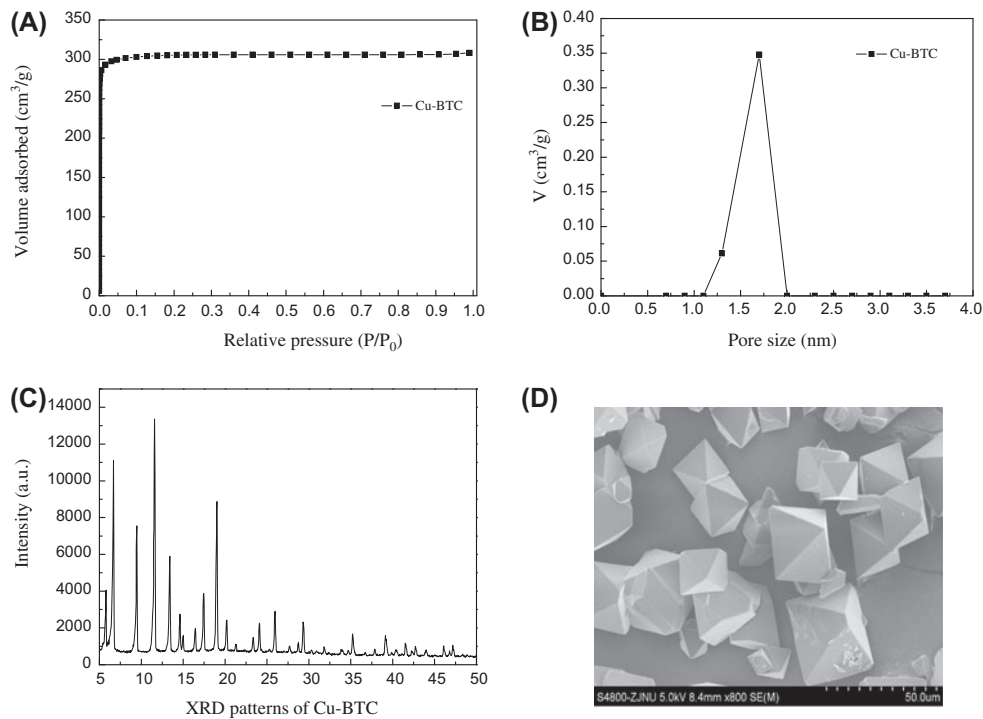


Fig. 2. Characterization of as-prepared Cu-BTC. (A) N_2 adsorption isotherms of Cu-BTC sample at 77 K, (B) pore size distribution of Cu-BTC sample, (C) XRD patterns of as-prepared Cu-BTC, and (D) SEM image of as-prepared Cu-BTC.

3.3. Adsorption isotherms

Isotherms study can describe how an adsorbate interacts with adsorbent. The isotherm provides a relationship between the concentration of dye in solution and the amount of dye adsorbed on the solid phase when both phases are in equilibrium. The adsorption isotherms of MB and CR at 303, 313, and 323 K on the Cu-BTC at a solid/liquid ratio of

0.4 g/L are presented in Figs. 4 and 5. Usually, the Langmuir isotherm is often applicable to a homogeneous adsorption surface with all the adsorption sites having equal adsorbate affinity, while the Freundlich isotherm is an empirical relation for adsorption over heterogeneous surfaces. The linear form of Langmuir's isotherm model [13] is given by the following equation:

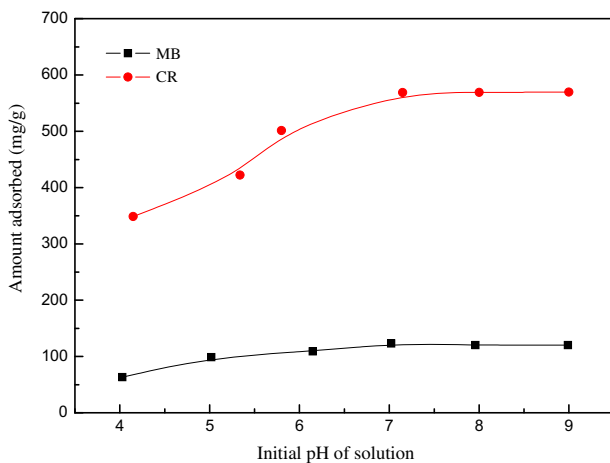


Fig. 3. Effect of solution pH on adsorption amounts of the dyes.

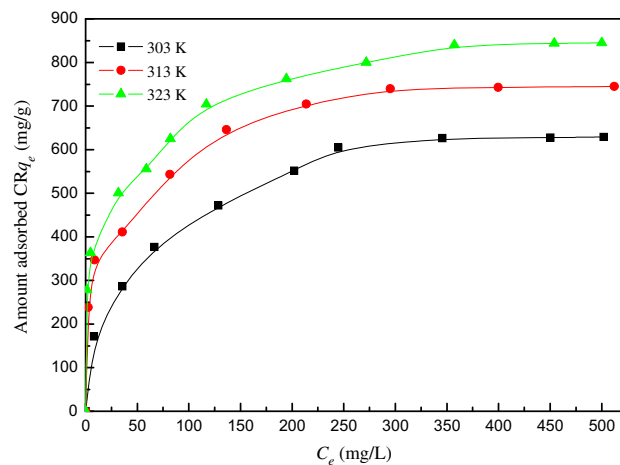


Fig. 4. Adsorption isotherms of CR on Cu-BTC at 303, 313, and 323 K, respectively.

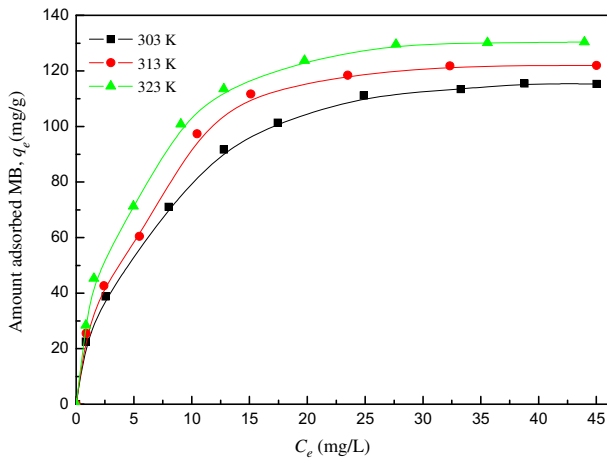


Fig. 5. Adsorption isotherms of MB on Cu-BTC at 303, 313, and 323 K, respectively.

$$\frac{C_e}{q_e} = \frac{1}{q_L \cdot K_L} + \left(\frac{1}{q_L}\right) \cdot C_e \quad (2)$$

where q_L (mg/g) is the Langmuir maximum uptake of MB and CR per unit mass adsorbent, K_L (L/mg) is the Langmuir constant related to the rate of adsorption.

The well-known logarithmic form of Freundlich model [14] is given by the following equation:

$$\ln q_e = \ln K_f + \left(\frac{1}{n}\right) \cdot \ln C_e \quad (3)$$

where K_f and n are Freundlich constants, with n indicating the favorableness of the adsorption process and K_f is the adsorption capacity of the adsorbent. K_f can be defined as the adsorption or distribution coefficient and its represents the quantity of dye adsorbed onto activated carbon adsorbent for a unit equilibrium concentration. The slope $1/n$ ranging between 0 and 1, is a measure of adsorption intensity or surface heterogeneity, becoming more heterogeneous as its value gets closer to zero.

The calculated constants according to the two isotherm equations along with R^2 values (standard deviation) are presented in Table 1. This table shows that the Langmuir isotherm gives the best fittings with $R^2 > 0.998$. The good fittings to the Langmuir model for the dyes also suggest that the adsorption is limited with a monolayer coverage and the surface is relatively homogeneous. On the other hand, for MB and CR dyes, the maximum monolayer adsorption capacity (q_L) is significantly higher on Cu-BTC and varies in

the order of $CR > MB$. The uptake capacity of CR is also significantly higher than that of the MB (approximately 6.1-fold higher). This may be due to the different molecule sizes and function groups of the two dyes. The result suggested that adsorption mechanism was monolayer coverage on the surface of the adsorbent [2]. In addition, the values of q_0 evaluated from Langmuir model were close to the experimental values of q_e . The adsorption capacities of MB and CR on Cu-BTC in this work are summarized in Table 2, together with those of the other MOFs and adsorbents. It is clear that the adsorption capacity of Cu-BTC is superior to the other previously reported adsorbents [15–18].

3.4. Adsorption kinetics

Adsorption kinetics was mainly used to investigate diffusion mechanism, adsorbed control step, and influencing factors of adsorbed velocity [18,19]. The adsorption data were fitted to the pseudo-first-order kinetic model and the pseudo-second-order kinetic model, respectively. The procedure used for kinetic tests was identical to that used for equilibrium experiments. Pseudo-first-order model [20], pseudo-second-order model [21], and intra-particle diffusion model [22] were used to analyze the kinetic data. These models can be expressed as:

$$\text{Pseudo-first order model: } \ln (q_e - q_t) = \ln (q_e) - K_1 t \quad (4)$$

$$\text{Pseudo-second order model: } \frac{t}{q_t} = \frac{1}{K_2 q_e} + \frac{t}{q_e} \quad (5)$$

$$\text{Intra-particle diffusion model: } q_t = K_3 t^{1/2} \quad (6)$$

where q_e and q_t (mg/g) are the uptake of MB and CR at equilibrium and at time t (min), respectively, K_1 (1/min) is the adsorption rate constant, K_2 (g/mg min) is the rate constant of second-order equation, K_3 (mg/g.min^{1/2}) is the intra-particle diffusion rate constant.

In order to quantitatively compare the applicability of different kinetic models in fitting to data, a normalized standard deviation, Δq (%), was calculated as below:

$$\Delta q (\%) = \frac{(q_{e,exp} - q_{e,cal})}{q_{e,exp}} \times 100\% \quad (7)$$

The effect of contact time on adsorption capacity of Cu-BTC to MB and CR at different temperatures is

Table 1
Constants and correlation coefficients of Langmuir and Freundlich

Dye	Temperature (K)	Langmuir			Freundlich		
		q_L (mg/g)	K_L (L/mg)	R^2	K_f (L/g)	n	R^2
MB	303	130.7190	0.1875	0.9986	26.6806	2.3486	0.9824
	313	137.7410	0.2111	0.9969	29.8884	2.3641	0.9746
	323	143.2665	0.2727	0.9991	36.4999	2.5971	0.9699
	303	689.6552	0.0223	0.9981	90.6848	3.0417	0.9886
CR	313	775.1938	0.0488	0.9986	203.0820	4.5179	0.9891
	323	877.1930	0.0467	0.9984	267.3397	5.2154	0.9958

Table 2
Comparison of the maximum adsorption capacities of MB and CR dyes on various adsorbents

Dye	Adsorbent	Maximum adsorption capacities (mg/g)	References
MB	Cu-BTC	143.27	This work
	HKUST-1/GO	140.00	[15]
	MIL-101	21.00	[16]
	Nem leaf powder	19.61	[23]
	Cu-BTC	877.19	This work
CR	Glu-Cu ²⁺ (MOFs)	77.60	[17]
	MFe ₂ O ₄	170.00	[18]
	Coir pith	6.72	[23]

shown in Figs. 5 and 6, respectively. The calculated constants of the three kinetic equations along with R^2 values at different temperatures are presented in Table 3. There is a large difference between the experimental and calculated adsorption capacity values when the pseudo-first-order model was applied. However, high R^2 values (0.99) are obtained with the linear

plot of t/q_t versus t , suggesting that the adsorption process followed a pseudo-second-order kinetic model. According to intra-particle diffusion model, a plot of the amount of dye adsorbed (q_t) versus the square root of time ($t^{1/2}$) should be linear, and if these lines pass through the origin, then the intra-particle diffusion is the only rate-controlling step [23].

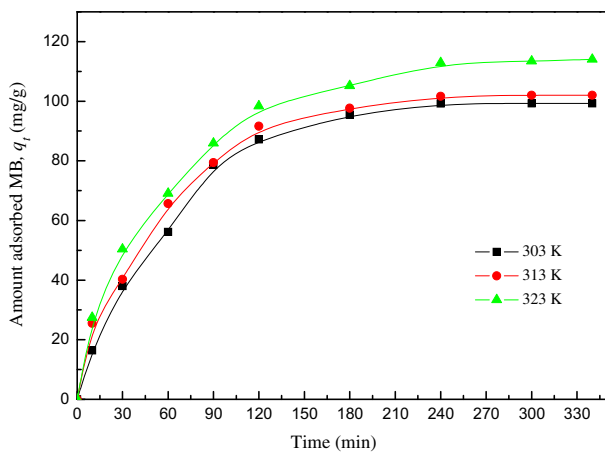


Fig. 6. Effect of contact time on the adsorption capacity of MB at different temperature.

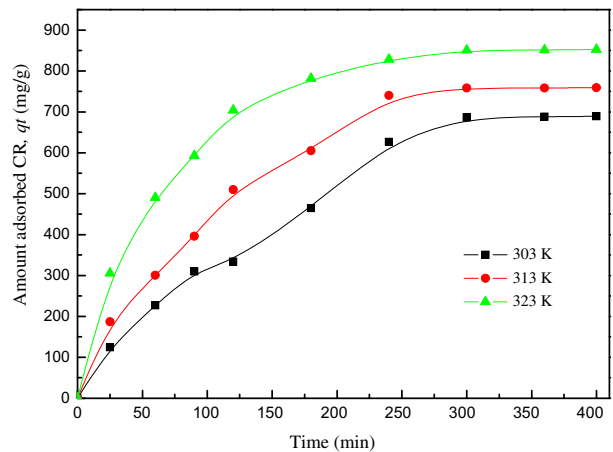


Fig. 7. Effect of contact time on the adsorption capacity of CR at different temperature.

Table 3
Kinetic parameters for MB and CR adsorption on Cu-BTC

Temperature (K)	Dye	Pseudo-first-order rate equation				Pseudo-second-order rate equation				Intra-particle diffusion model							
		$q_{e,exp}$ (mg/g)	$q_{e,cal}$ (mg/g)	K_1 (1/min)	R^2	Δq (mg/g)	Δq (%)	$q_{e,exp}$ (mg/g)	$q_{e,cal}$ (mg/g)	K_2 (g/mg min)	R^2	Δq (mg/g)	Δq (%)	$q_{e,exp}$ (mg/g)	C (mg/g)	K_3 (mg/g min ^{1/2})	R^2
303	MB	99.30	195.77	0.028	0.9509	-96.47	-97.15	99.30	131.06	0.0143	0.9956	-31.76	-31.98	99.30	13.75	5.381	0.9324
	CR	688.15	2297.22	0.020	0.9389	-1609.07	-233.83	688.15	1282.05	0.0036	0.9851	-593.9	-86.30	688.15	-111.05	44.22	0.9887
313	MB	101.65	132.91	0.022	0.9788	-31.26	-30.75	101.65	123.61	0.0203	0.9956	-21.96	-0.18	101.65	21.41	5.057	0.9336
	CR	758.32	2376.73	0.023	0.9563	-1618.41	-213.42	758.32	1162.79	0.0064	0.9858	-404.47	-53.33	758.32	-18.22	44.72	0.9814
323	MB	113.42	123.88	0.018	0.9882	-10.46	-9.22	113.42	134.23	0.0209	0.9976	-20.81	-18.35	113.42	23.38	5.579	0.9512
	CR	851.27	1690.26	0.022	0.9426	-838.99	-98.55	851.27	1041.66	0.0160	0.9991	-190.39	-22.37	851.27	198.50	38.78	0.9499

However, the plots are not linear over the whole time range and, instead, can be separated into multi-linear curves, illustrating that multiple stages were involved in the adsorption process. The results indicated that the adsorption of MB and CR dyes onto Cu-BTC involved more than one process, and the intra-particle transport is not the rate-limiting step. Such finding is similar to that made in previous works on adsorption [24,25].

3.5. Adsorption thermodynamics

Thermodynamic behavior of MB and CR adsorption onto Cu-BTC was evaluated by the thermodynamic parameters including the changes in free energy (G), enthalpy (H), and entropy (S). These parameters are calculated from the following equations:

$$\ln(K_d) = \frac{\Delta S}{R} - \frac{\Delta H}{RT} \quad (8)$$

$$\Delta G = -RT \ln(K_d) \quad (9)$$

$$K_d = \frac{q_e(W/V)}{C_e} \quad (10)$$

where R is the universal gas constant 8.314 (J/mol K), T is the temperature (K), and K_d is the distribution coefficient for the adsorption.

On the basis of the MB and CR adsorption isotherm data which were calculated from Eq. (1), the value of K_d was calculated from Eq. (10) at each temperature [26]. Then, according to Eqs. (8) and (9), the ΔH and ΔS parameters for MB and CR adsorption can be derived from the slope and intercepts of the plot of $\ln(K_d)$ versus $1/T$. The calculated values of ΔH , ΔS , and ΔG are listed in Table 4.

Temperature has a very significant influence on the adsorption process because the change in temperature will cause large changes in the adsorption equilibrium capacity of the adsorbent for a particular

adsorbate. Adsorption experiments were carried out at different temperatures (303, 313, 323 K) in order to investigate the effect of adsorption temperature on the adsorption capacity of MB and CR on Cu-BTC. As can be seen from Fig. 4–7, the dyes (MB and CR) adsorption capacities increased as the temperature increase from 303 to 323 K. As is known from Table 4, the ΔH parameters are positive for MB and CR adsorption on Cu-BTC, which indicate that higher temperature is favorable for adsorption. The negative ΔG values indicate thermodynamically the spontaneous nature of adsorption. The positive ΔS value suggests a compensation for the adsorption enthalpy to favor the adsorption thermodynamics.

In general, the adsorption enthalpy ranging from 2.1 to 20.9 kJ/mol corresponds to a physical adsorption [27]. In this study, the ΔH parameters are 5.91 and 20.32 kJ/mole for MB and CR adsorption on Cu-BTC, which is in the range of physical adsorption. However, physical adsorption is usually spontaneous and exothermic process [2]. The adsorption capacities of MB and CR on Cu-BTC increase with temperature, in this work is possible, which is controlled by various factors including physical and chemical properties and surface structure of Cu-BTC, molecular structure of dyes, hydrophobic interaction, electrostatic force, mass transfer process, competitive adsorption of H_2O molecular, etc. [28,29].

4. Conclusion

MB and CR dyes in contaminated water can be efficiently removed with Cu-BTC. It was more effective for removal of CR than MB. Batch adsorption tests demonstrate that the adsorption is affected by various conditions such as contact time, solution pH, and initial dye concentration. Adsorption kinetics follows the pseudo-second-order model. Equilibrium data are fitted by Langmuir and Freundlich isotherms and the equilibrium data are better described by Langmuir isotherm model, with maximum equilibrium adsorption capacity of 143.27 mg/g (MB) and 877.19 mg/g (CR), respectively. In basis of this study, it can be suggested that Cu-BTC may be applied in the adsorptive removal of dyes in the liquid phase.

Acknowledgments

This work was supported by the Public Projects of Zhejiang Province of China (No. 2013C31093), Zhejiang Qianjiang Talent Project (No. QJD1302015).

Table 4
Thermodynamics adsorption parameters for MB and CR on Cu-BTC

Dye	ΔH (kJ/mol)	ΔS (J/mol)	ΔG (kJ/mol)		
			303 K	313 K	323 K
MB	5.91	77.82	-17.69	-18.42	-19.25
CR	20.32	123.71	-16.16	-17.44	-18.63

References

- [1] J. Hu, H. Yu, W. Dai, X. Yan, X. Hu, H. Huang, Enhanced adsorptive removal of hazardous anionic dye “congo red” by a Ni/Cu mixed-component metal–organic porous material, *RSC Adv.* 4 (66) (2014) 35124–35130.
- [2] R. Gong, J. Ye, W. Dai, X. Yan, J. Hu, X. Hu, S. Li, H. Huang, Adsorptive removal of methyl orange and methylene blue from aqueous solution with finger-citron-residue-based activated carbon, *Ind. Eng. Chem. Res.* 52 (2013) 14297–14303.
- [3] B. Royer, N.F. Cardoso, E.C. Lima, J.C. Vaghetti, N.M. Simon, T. Calvete, R.C. Veses, Applications of Brazilian pine-fruit shell in natural and carbonized forms as adsorbents to removal of methylene blue from aqueous solutions—Kinetic and equilibrium study, *J. Hazard. Mater.* 164 (2009) 1213–1222.
- [4] S. Chatterjee, D.S. Lee, M.W. Lee, S.H. Woo, Congo red adsorption from aqueous solutions by using chitosan hydrogel beads impregnated with nonionic or anionic surfactant, *Bioresour. Technol.* 100 (2009) 3862–3868.
- [5] Y.M. Slokar, M.L. Marechal, Methods of decoloration of textile wastewaters, *Dyes Pigment.* 37 (1998) 335–356.
- [6] P. Vandevivere, R. Bianchi, W. Verstraete, Treatment and reuse of wastewater from textile wet-processing industry: Review of emerging technologies, *J. Chem. Technol. Biotechnol.* 72 (1998) 289–302.
- [7] A.R. Millward, O.M. Yaghi, Metal-organic frameworks with exceptionally high capacity for storage of carbon dioxide at room temperature, *J. Am. Chem. Soc.* 127 (2005) 17998–17999.
- [8] K.A. Cychosz, A.G. Wong-Foy, A.J. Matzger, Liquid phase adsorption by microporous coordination polymers: Removal of organosulfur compounds, *J. Am. Chem. Soc.* 130 (2008) 6938–6939.
- [9] G. Blanco-Brieva, J.M. Campos-martin, S.M. Al-zahrani, J.L.G. Fierro, Removal of refractory organic sulfur compounds in fossil fuels using mof sorbents, *Global Nest J.* 12 (2010) 296–304.
- [10] S.S.Y. Chui, S.M.F. Lo, J.P.H. Charmant, A.G. Orpen, I.D. Williams, A chemically functionalizable nanoporous material $[\text{Cu}_3(\text{TMA})_2(\text{H}_2\text{O})_3]_n$, *Science* 283 (1999) 1148–1150.
- [11] Z. Xiang, X. Peng, X. Cheng, X. Li, D. Cao, $\text{CNT}@\text{Cu}_3(\text{BTC})_2$ and metal-organic frameworks for separation of CO_2/CH_4 mixture, *J. Phys. Chem. C* 115 (2011) 19864–19871.
- [12] W. Dai, R. Gong, J. Hu, L.M. Zhou, Thiophene capture by an oxidation-modified activated carbon derived from bergamot, *Sep. Sci. Technol.* 49 (2014) 367–375.
- [13] I. Langmuir, The constitution and fundamental properties of solids and liquids, *J. Am. Chem. Soc.* 38 (1916) 2221–2295.
- [14] H.M.F. Freundlich, Über die adsorption in losungen, *Z. Phys. Chem.* 57 (1906) 385–470.
- [15] L. Li, X. Liu, H. Geng, B. Hu, G. Song, Z. Xu, A MOF/graphite oxide hybrid (MOF: HKUST-1) material for the adsorption of methylene blue from aqueous solution, *J. Mater. Chem.* 1 (2013) 10292–10299.
- [16] X. Huang, L. Qiu, W. Zhang, Y. Yuan, X. Jiang, A. Xie, Y. Shen, J. Zhu, Hierarchically mesostructured MIL-101 metal–organic frameworks: Supramolecular template-directed synthesis and accelerated adsorption kinetics for dye removal, *Cryst. Eng. Comm.* 14 (2012) 1613–1617.
- [17] F. Pu, X. Liu, B. Xu, J. Ren, X. Qu, Miniaturization of metal-biomolecule frameworks based on stereoselective self-assembly and potential application in water treatment and as antibacterial agents, *Chem. Eur. J.* 18 (2012) 4322–4328.
- [18] L. Wang, J. Li, Y. Wang, L. Zhao, Q. Jiang, Adsorption capability for congo red on nanocrystalline MFe_2O_4 ($\text{M} = \text{Mn}, \text{Fe}, \text{Co}, \text{Ni}$) spinel ferrites, *Chem. Eng. J.* 181–182 (2012) 72–79.
- [19] Z. Liu, A. Zhou, G. Wang, X. Zhao, Adsorption behavior of methyl orange onto modified ultrafine coal powder, *Chin. J. Chem. Eng.* 17 (2009) 942–948.
- [20] E. Haque, J.W. Jun, S.H. Jhung, Adsorptive removal of methyl orange and methylene blue from aqueous solution with a metal-organic framework material, iron terephthalate (MOF-235), *J. Hazard. Mater.* 185 (2011) 507–511.
- [21] J. Yang, K. Qiu, Preparation of activated carbons from walnut shell via vacuum chemical activation and their application for methylene blue removal, *Chem. Eng. J.* 165 (2010) 209–217.
- [22] M. Vinoth, H.Y. Lim, R. Xavier, K. Marimuthu, S. Sreeramanan, H.M.H. Rosemal, S. Kathiresan, Removal of methyl orange from solutions using yam leaf fibers, *Int. J. Chem. Technol. Res.* 2 (2010) 1890–1900.
- [23] K.G. Bhattacharyya, A. Sharma, Kinetics and thermodynamics of methylene blue adsorption on neem (*Azadirachta indica*) leaf powder, *Dyes Pigment.* 65 (2005) 51–59.
- [24] S. Chatterjee, D.S. Lee, M.W. Lee, S.H. Woo, Enhanced adsorption of congo red from aqueous solutions by chitosan hydrogel beads impregnated with cetyl trimethyl ammonium bromide, *Bioresour. Technol.* 10 (2009) 2803–2809.
- [25] L.C. Juang, C.C. Wang, C.K. Lee, Adsorption of basic dyes onto MCM-41, *Chemosphere* 64 (2006) 1920–1928.
- [26] S. Karagoz, T. Tay, S. Ucar, M. Erdem, Activated carbons from waste biomass by sulfuric acid activation and their use on methylene blue adsorption, *Bioresour. Technol.* 99 (2008) 6214–6222.
- [27] Z. Belala, M. Jeguirim, M. Belhachemi, F. Addoun, G. Trouvé, Biosorption of basic dye from aqueous solutions by date stones and palm-trees wastes: Kinetic, equilibrium and thermodynamic studies, *Desalination* 271 (2011) 80–87.
- [28] J. Yi, L. Zhang, Removal of methylene blue dye from aqueous solution by adsorption onto sodium humate/polyacrylamide/clay hybrid hydrogels, *Bioresour. Technol.* 99 (2008) 2182–2186.
- [29] V. Rocher, J. Siaugue, V. Cabuil, A. Bee, Removal of organic dyes by magnetic alginatebeads, *Water Res.* 42 (2008) 1290–1298.